The application of Co–Al-hydrotalcite as a novel additive of positive material for nickel–metal hydride secondary cells

CrossMark

Zhaobin Feng [a], Zhanhong Yang [a,b,*], Bin Yang [a,b], Zheng Zhang [a], Xiaoe Xie [a]

[a] College of Chemistry and Chemical Engineering, Central South University, Changsha 410083, China
[b] Key Laboratory of Resource Chemistry of Nonferrous Metals, Ministry of Education, Central South University, Changsha 410083, China

HIGHLIGHTS

- Co–Al-hydrotalcites were proposed as additive of positive material for Ni–MH secondary cells for the first time.
- The additive Co–Al-hydrotalcites have a significantly improved the electron conductivity.
- Ni–MH cells with Co–Al-hydrotalcites as additive have superior electrochemical cycle stability.
- The sample of Co/Al = 4/1 (molar ration) as additive exhibits best electrochemical properties.

ARTICLE INFO

ABSTRACT

Co–Al–CO$_3$ layered double hydroxide (LDH) with the different Co/Al molar ration is synthesized by hydrothermal method and investigated as an additive for positive material of the Ni–MH cells. The Fourier transform infrared spectra (FT-IR), scanning electron microscopy (SEM) and X-ray diffraction (XRD) show the Co–Al-LDH with Co/Al = 4:1 (molar ration) is well-crystallized and hexagon structure. The electrochemical performances of the nickel electrode added with different Co/Al molar ration Co–Al-LDH, the pure nickel electrode and the nickel electrode added with CoO are investigated by the cyclic voltammograms (CV), galvanostatic charge–discharge measurements, and AC electrochemical impedance spectroscopy (EIS). Compared with the pure nickel electrode and the nickel electrode added with CoO, the nickel electrode added with Co/Al = 4:1 (molar ration) Co–Al-LDH has higher discharge capacity and more stable cycling performances. This cell can undergo at least 400 charge–discharge cycles at constant current of 1 C. The discharge capacity of this cell remains about 287 mAh g^{-1} after the 400th cycle. Meanwhile, compared with the pure electrode, the nickel electrode added with Co/Al = 4:1 (molar ration) Co–Al-LDH possess a higher rate capability to meet the needs of high-storage applications.

© 2014 Elsevier B.V. All rights reserved.

1. Introduction

There has been a rising interest in the research about Ni–MH alkaline secondary battery for its advantages in high power density, smooth discharge platform, high specific energy, environment non-toxicity and good low-temperature performance. These advantages also make it to be one of the most promising devices for electric vehicle (EV) and hybrid electric vehicle (HEV) applications. As we all known, a power battery has to satisfy some essential requirements, the most important is the low internal resistance of the active

materials [1]. However, the poor conductivity of β-Ni(OH)$_2$ [2] hampers the widespread application as an active material for Ni–MH batteries. And, during the cell cycle, the γ-NiOOH formation shortens the cycle life of the batteries. For decades, many efforts have been made to solve the problems mentioned above. A large variety of inorganic additives, such as Cd(OH)$_2$ [3], Zn(OH)$_2$ [4,5], Mn^{2+} [5,6], calcium compounds [5,7,8], and Y(OH)$_3$ [9,10] have been adopted in the nickel electrode to overcome these difficulties. Especially, cobalt compounds are considered to be important component of the nickel electrode because these compounds have the abilities to restrain the formation of γ-NiOOH and O$_2$, decrease the charge-transfer resistance [11,12], increase the conductivity of proton, improve the depth of discharge and efficiency of charge–discharge [13]. Hence, Cobalt and its hydroxides and oxides [10,14–21] have been studied in many ways, Yang et al. [21] use core–shell

* Corresponding author. College of Chemistry and Chemical Engineering, Central South University, Changsha 410083, China. Tel./fax: +86 0731 88879616.
E-mail address: zhongnan320@gmail.com (Z. Yang).

Ni(OH)@CoOOH to improve conductivity of the nickel electrode. Despite the many advantages, cobalt can be reduced and tends to move to the surface of a current collector. It decreases the cell performance when the cell is stored in the discharge state [1]. Thus, it is necessary to construct the stable conductive network in the nickel electrode.

LDH has the advantage in low cost, relatively environment friendly nature and the excellent electrochemical properties. It has been studied in the field of being new modified electrodes. Among these LDH, Zn–Al-LDH, Zn–Al-La-LDH and Zn–Al–In-LDH employed as novel anodic material for Zn–Ni secondary cell had been investigated by our group [22–24]. Co–Al-LDH, as a kind of cobalt compound, is not easily destroyed in the alkaline solution. Thus it can be an additive for positive material of Ni–MH battery and improve the electrochemical properties of the electrode. However, it is rarely studied in the field of Ni–MH battery. In this paper, Co–Al-LDH, synthesized by hydrothermal method, is being used an additive for positive material of the Ni–MH battery. Material characterization studies on Co–Al-LDH with different Co/Al molar rations and electrochemical measurements on the nickel electrodes added with different Co/Al molar rations Co–Al-LDH were also carried out.

2. Experimental

2.1. The preparation of Co–Al-LDH

Co–Al-LDH was prepared by the method of hydrothermal. The typical experimental operation was as follows: $Al(NO_3)_3 \cdot 9H_2O$ (AR, Guangdong city Guanghua Fine Chemical Institute) blended with $CoSO_4 \cdot 7H_2O$ (AR, Shantou city Hongwei Fine Chemical Research Institute) was dissolved in the deionized water solution; then the above saline solution and a mixture containing NaOH (AR, Xilong Chemical Industry) and Na_2CO_3 (AR, Jiangsu province Qiangshen Chemical Industry) were added simultaneously to a beaker at a speed of 1 drop s^{-1}. The process was carried out under a constant pH = 10 and vigorous stirring at the 65 °C. After stirring for 30 min, the mixed solution was transferred to an autoclave pressure vessel and heated at 180 °C for 10 h. After filtered and washed with distilled water and ethanol, the precipitate was dried and ground to fine power. In this paper, Co–Al-LDH with Co/Al (molar ration) = 3:1, 4:1, 5:1 are coded A, B and C, respectively.

2.2. The characterization of the Co–Al-LDH

Fourier transform infrared (FT-IR) spectra were performed on a Nicolet AVATAR-360 FT-IR spectrometer with wave number 400–4000 cm^{-1} using KBr pellet technique. XRD patterns of samples were carried out by a D500 (Siemens) diffractometer (36 kV, 30 mA) using Cu Kα radiation. The morphology of the Co–Al-LDH products was conducted by SEM (Quanta FEG 250).

2.3. The preparation of the nickel electrodes

The nickel electrodes added with Co–Al-LDH were prepared by pasting a mixture containing as-prepared Co–Al-LDH, spherical β-nickel hydroxide, acetylene black, carboxymethyl cellulose sodium (CMC, in diluted emulsion) and polytetrafluoroethylene (PTFE, in diluted emulsion) on a foam nickel substrate(1.0 cm × 1.0 cm in size). The weight ratio of Co–Al-LDH, spherical β-nickel hydroxide, acetylene black, CMC and PTFE was 10:86:2:1:1. To ensure the same amounts of Cobalt element, the nickel electrode added with CoO is comprised of 5.7% CoO, 90.3% spherical β-nickel hydroxide, 2% acetylene black, 1% CMC and 1% PTFE. Then, the obtained nickel electrodes were pressed to a thickness of 0.3 mm and dried at 65 °C

under vacuum. In order to compare with the nickel electrode added with Co–Al-LDH, the pure nickel electrode was also prepared by the same way.

2.4. The electrochemical characterization of the electrodes

Firstly, all the cells were pre-activated for 5 times. During the pre-activated procedure, the cells were charged at 0.1 C for 10 h and discharged at 0.2 C down to 0.9 V cutoff voltage. Then, the cyclic voltammetry and the electrochemical impedance spectroscope measurements were conducted in a conventional three-electrode at room temperature (25 ± 1 °C) using a Hg/HgO as the reference electrode, a nickel electrode as the working electrode, and a hydrogen storage alloy electrode as the counter electrode. The electrolyte was 6 M KOH solution. The cyclic voltammetry measurements were performed on a RST-5000 type electrochemical system with a scanning rate of 5.0 mV s^{-1}, shifting from 0.1 V to 0.65 V. The AC-Impedance measurements were fulfilled on a PAR-STAT 2273-type electrochemical system (Princeton Applied Research) with a frequency range between 0.01 Hz and 100 kHz, the AC signal amplitude is 5 mV.

At room temperature (25 ± 5 °C), the galvanostatic charge–discharge tests were performed on a BTS-5 V/100 mA battery-testing instrument (Neware, China). The test cells included the hydrogen storage alloy electrode as counter electrode and the nickel electrode as working electrode. They were circularly charged under the condition of 2.5 V, and then discharged to 0.9 V cutoff.

To investigate the rate performance of the cells, firstly, the cells were charged at 0.1 C and discharged at 0.2 C for five cycles in the active process. Then, to guarantee the stability of the cell, the cells were charged at 1 C and discharged at 1 C for forty-five cycles. Last, the cells were charged at 1 C and discharged at 0.5 C, 1 C, 2 C and 5 C for ten cycles, respectively.

3. Results and discussion

3.1. FT-IR analysis of Co–Al-LDH

Fig. 1 shows FT-IR spectra of the Co–Al-LDH with the different Co/Al molar ration. As seen in Fig. 1, the FT-IR spectra for sample A, sample B and sample C are very similar. The broad peak around
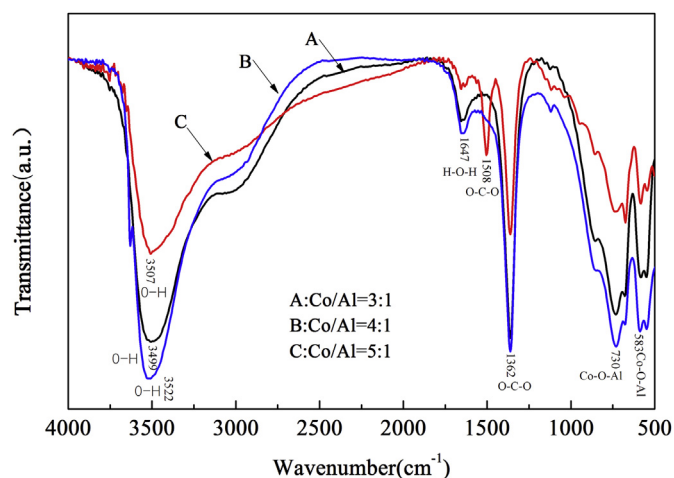

Fig. 1. FT-IR spectra for the Co–Al-LDH with the different Co/Al molar ration. A: Co/Al = 3:1; B: Co/Al = 4:1; C: Co/Al = 5:1.

3520 cm^{-1} can be attributed to the stretching of OH$^-$ attached to metal ions. The peak of the bending vibration of interlayer appears at 1647 cm^{-1}. The O—C—O asymmetric stretching vibration is founded at 1508 cm^{-1} and 1362 cm^{-1}. The lower shifted absorption peak at 1362 cm^{-1}, as compared with CO_3^{2-} of $CaCO_3$ (1430 cm^{-1}), shows that there is an intercalation between CO_3^{2-} and interlayer H_2O through the strong hydrogen bonding [23]. The peaks appearing between 400 cm^{-1} and 750 cm^{-1} are ascribed to the vibration of Co—Al-LDH lattice (Al—O, Co—O).

3.2. The XRD and SEM analysis for Co—Al-LDH

Fig. 2a shows the typical SEM image for Co/Al = 4:1 (molar ration) Co—Al-LDH. As seen in Fig. 2a, the existing lamellar has a hexagonal shape which is the typical structure of the hydrotalcite-like material. Fig. 2b shows XRD patterns of the Co—Al-LDH with the different Co/Al molar ration. As seen from Fig. 2b, the diffraction peaks (at 2θ = 11.5°, 23.8°, 38.6° and 61.7°) of sample B are accordingly corresponding to the relations of (003), (006), (009) and (110). The diffraction peaks which are narrow, sharp and symmetrical suggest that the sample is well-crystallized. Meanwhile, the strongest diffraction peak which appears at 2θ = 11.5° indicates the Co—Al-LDH crystals grow along the (003) and develop a typical hexagonal crystal structure like hydrotalcite compound. The diffraction peaks of sample A are similar to sample B. But there are some differences among them. The diffraction peaks of sample A are less sharp than sample B. It indicates the crystallinity of sample B is better to sample A. The diffraction peaks of sample C are quite different from sample A and sample B, excepting 2θ = 11.5°, 23.8°. It suggests sample C is able to develop the hexagonal crystal structure but has many other substances. Thus, the Co—Al-LDH with Co/Al = 4:1 has high crystallinity and integrated crystalline structures.

3.3. The cyclic voltammetry (CV) of the different nickel electrodes

In order to understand the effects of the additive Co—Al-LDH on the electrochemical performance of the nickel electrode, CV studies were conducted. Fig. 3 shows the cyclic voltammograms of the nickel electrodes added with different Co/Al molar ratio Co—Al-LDH, the pure nickel electrode and the nickel electrode added with CoO. In Fig. 3, the nickel electrodes added with Co—Al-LDH whose Co/Al (molar ration) is 3/1, 4/1 and 5/1, respectively, are coded the electrode A, B and C, the pure nickel electrode is coded the electrode D and the nickel electrode added with CoO is coded the electrode E.

As seen from Fig. 3, the potential sweep starts from 0.6 V along the direction of cathode. On the first cathodic scan, the cathodic peak potential of the nickel electrodes added with Co—Al-LDH is more positive than the pure nickel electrode. In general, a little more positive potential means a higher electrochemical kinetics of the reduction process [25]. Thus, the nickel electrodes added with Co—Al-LDH have a better reduction process. The reason for the potential difference between the nickel electrodes added with Co—Al-LDH and the pure nickel electrode is that the CoOOH is formed in the activity process and improves the conductivity of the nickel electrodes. When the nickel electrodes added with Co—Al-LDH are immersed into electrolyte, the cobalt ion is able to be transformed into $Co(OH)_4^{2-}$. Then, the $Co(OH)_4^{2-}$ is oxidized into CoOOH in the
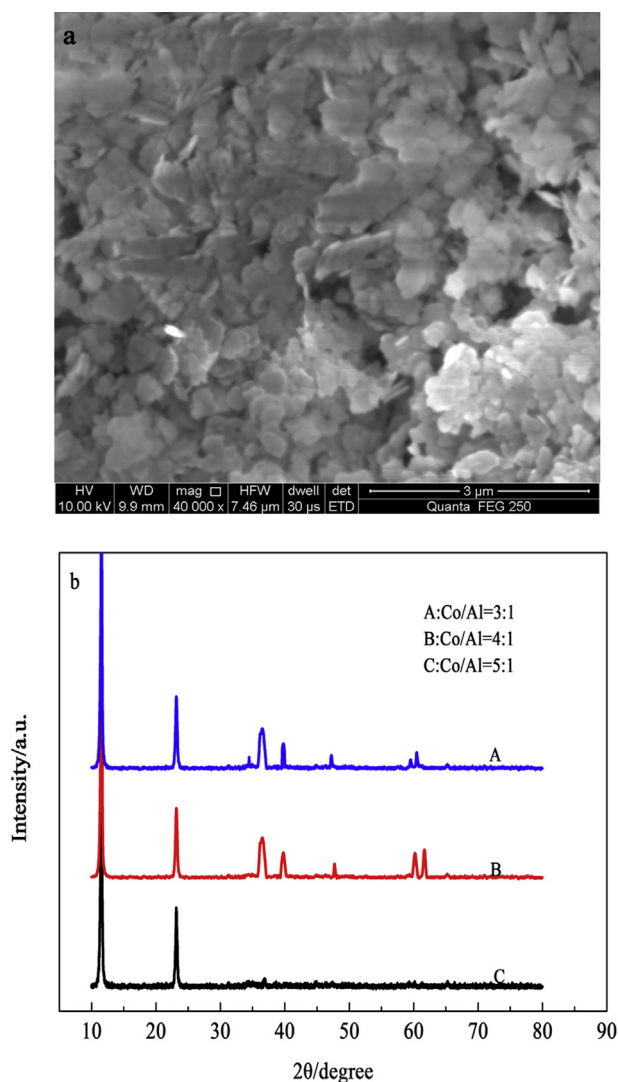

Fig. 2. (a) Typical SEM image for Co—Al-LDH with Co/Al = 4:1 (molar ration). (b) XRD patterns for the Co—Al-LDH with the different Co/Al molar ration. A: Co/Al = 3:1 (molar ration); B: Co/Al = 4:1 (molar ration); C: Co/Al = 5:1 (molar ration).
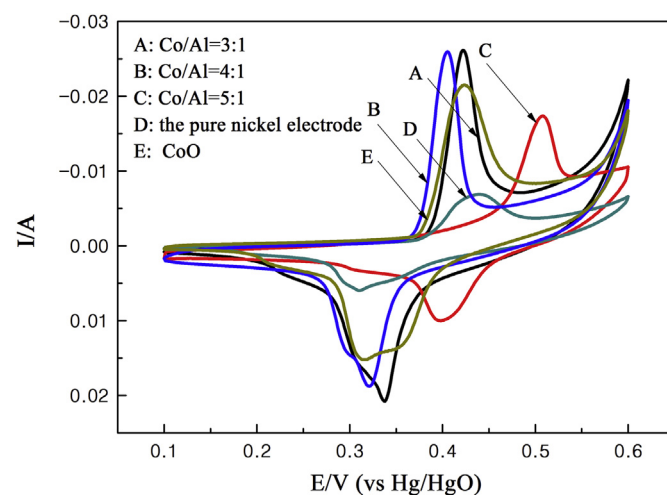

Fig. 3. Cyclic voltammograms for the nickel electrodes: (A) the nickel electrode added with Co/Al = 3:1 (molar ration) Co—Al-LDH; (B) the nickel electrode added with Co/Al = 4:1 (molar ration) Co—Al-LDH; (C) the nickel electrode added with Co/Al = 5:1 (molar ration) Co—Al-LDH; (D) the pure nickel electrode and (E) the nickel electrode added with CoO.

activity charge process. The reaction equations in the activated charge process are as follows:

$$Co(OH)_4{}^{2-} = CoOOH + H_2O + OH^- + e \tag{1}$$

$$Ni(OH)_2 + OH^- = NiOOH + H_2O + e \tag{2}$$
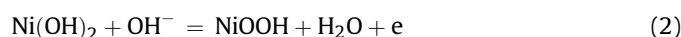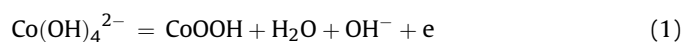
The Nernst equations of Eqs. (1) and (2) are, respectively,

$$\varphi_1 = \varphi^\theta_{Co^{3+}/Co^{2+}} + 0.0592 \lg \frac{[OH^-]}{\left[Co(OH)_4^{2-}\right]} \tag{3}$$

$$\varphi_2 = \varphi^\theta_{Ni^{3+}/Ni^{2+}} + 0.0592 \lg \frac{1}{[OH^-]} \tag{4}$$

The standard electrode potential of the Co^{3+}/Co^{2+} redox couple and the Ni^{3+}/Ni^{2+} redox couple is 0.17 V, 0.52 V, respectively. The calculation shows φ_1 is smaller than φ_2. Thus, $Co(OH)_4{}^{2-}$ firstly is oxidized into CoOOH in the activation charge process. And, CoOOH cannot be reduced during the subsequent discharge process [26]. In addition, because the hexagon structure of Co–Al-LDH is similar to β-Ni(OH)$_2$, Co–Al-LDH which convert to complex ion in strong alkaline solution is able to form the cocrystallization with Ni(OH)$_2$ in the activation process. It makes cobalt compound well disperse on the surface of β-Ni(OH)$_2$. Moreover, the conductivity of CoOOH is better than β-Ni(OH)$_2$ [27,28]. Thus, in the cathodic process, the converted CoOOH offers a good electrical path between the β-Ni(OH)$_2$ particles and the foamed-Ni substrate, is helpful to transfer electron in nickel electrode, improves the reaction rate of the limited Eq. (5), decreases the polarization and makes the potential move in the positive direction.

$$NiOOH + H_2O + e \rightarrow Ni(OH)_2 + OH^- \tag{5}$$
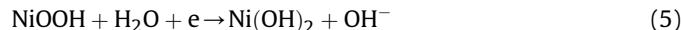
Thus, the overpotential of the nickel electrode added with Co–Al-LDH is smaller than the pure nickel electrode in the cathodic process.

When the potential scan turns to the more positive region, the anodic peak of the electrode A and B appears at 0.422 V and 0.405 V, respectively, which is moved in the more negative direction in comparison with the pure nickel electrode (0.439 V). The reaction equation in the oxidation process is as follows:

$$Ni(OH)_2 + OH^- \rightarrow NiOOH + H_2O + e \tag{6}$$
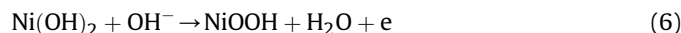
The lower potential indicates a higher electrochemical kinetics for the oxidation process. The possible reason is that the added Co–Al-LDH contributes to accelerating diffusion of OH^-. It is helpful to improve the reaction rate of Eq. (6) and decreases the polarization for the anodic process. Thus, the potential of anodic peak for the electrode A and B are more negative than the pure nickel electrode. Meanwhile, the current of anodic peak for the electrode A and B is higher than the pure nickel electrode, which also implies the high oxidation activity for the electrode A and B.

The potential interval ($\Delta E_{a,c}$) between an anodic peak and a cathodic peak is taken as a measurement of the reversibility of the electrode reaction, the smaller the interval, the better the reversibility [24].The $\Delta E_{a,c}$ for the electrode A, B, and C is 0.086 V, 0.085 V, and 0.11 V, respectively, which is smaller than the D electrode (0.13 V). Thus, the reversibility of the nickel electrode added with Co–Al-LDH is best among the nickel electrodes.

Meanwhile, as seen from Fig. 3, the reversibility of the nickel electrode added with Co/Al = 4:1 (molar ration) Co–Al-LDH is better than the nickel electrode added with CoO. The main reason is that Co–Al-LDH has a large number of OH^- and can accelerate diffusion of OH^-. In the cathodic process, the better diffusion of

OH^- makes the concentration of OH^- decrease around the NiOOH, promotes the positive moving of Eq. (5), decreases the polarization and makes the potential move in the positive direction. In the anodic process, the better diffusion of OH^- is also helpful to improve the reaction rate of Eq. (6), speeds up the electronic production, decreases the polarization and makes the potential move in the negative direction. Thus, the nickel electrode added with Co/Al = 4:1 (molar ration) Co–Al-LDH has the better reversibility.

3.4. The galvanostatic charge and discharge properties of Ni–MH cells with the different nickel electrodes

Fig. 4 displays the typical galvanostatic charge/discharge curves for the nickel electrodes added with different Co/Al molar ratios Co–Al-LDH, the pure nickel electrode and the nickel electrode added with CoO at the 25th cycle.

As shown in Fig. 4a, the nickel electrodes added with the Co–Al-LDH show a lower charge voltage platform than the pure nickel electrode which demonstrates that Co–Al-LDH is conducive to improving the charge conversion efficiency. It results from the existing of CoOOH improves the conductivity for the nickel electrodes. In other words, the nickel electrodes added with Co–Al-
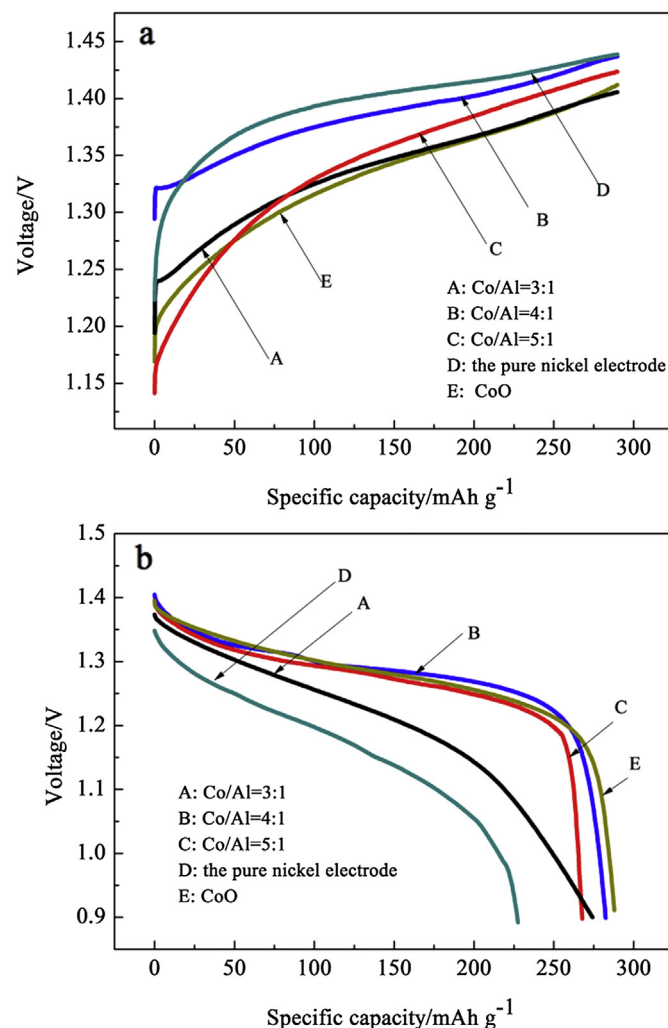

Fig. 4. Typical galvanostatic charge curves (a) and discharge curves (b) for the Ni–MH cells with: (A) the nickel electrode added with Co/Al = 3:1 (molar ration) Co–Al-LDH; (B) the nickel electrode added with Co/Al = 4:1 (molar ration) Co–Al-LDH; (C) the nickel electrode added with Co/Al = 5:1 (molar ration) Co–Al-LDH; (D) the pure nickel electrode and (E) the nickel electrode added with CoO at the 25th cycle.

LDH have small internal resistance, which can decrease the ohmic polarization and then make voltage fall. The voltage decreasing velocity of the electrodes is: electrode A > electrode C > electrode B. Although, the voltage decreasing velocity of the electrode B is smallest, the charge platform is more stable. It may be explained by the fact that the additive Co/Al = 4:1 (molar ration) Co–Al–LDH has complete hexagon layer structure as is shown in Fig. 2b. The complete hexagon layer structure is in favor of the OH⁻ transfer and improves the utilization of Ni(OH)$_2$. Meanwhile, Fig. 4a shows the charge voltage platform of the nickel electrode added with CoO is lower than the nickel electrode added with Co/Al = 4:1 (molar ration) Co–Al–LDH. But the stability of the former is not as good as the latter.

As seen in Fig. 4b, the discharge voltage platforms of the nickel electrodes added with Co–Al–LDH show the higher discharge voltage platform than the pure nickel electrode. It means the nickel electrodes added with Co–Al–LDH have higher working voltage. The main reason is that the exists of CoOOH, which stems from Co(OH)$_4^{2-}$, has better conductivity than NiOOH [10,29,30], provides a good electrical path between the NiOOH particles and the foamed-Ni substrate and decreases the internal resistance of the nickel electrode. For the Ni–MH cell, in the discharge process, the voltage can be calculated by the equation as follows:

$$E = E_+ - E_- - IR \qquad (7)$$

As the cyclic voltammetry (Fig. 3) shows, the cathodic polarization for the nickel electrode added with Co–Al–LDH is smaller than the pure nickel electrode. So the potential for the nickel electrodes added with Co–Al–LDH is more positive under the condition of the same current. According to Eq. (7), the lower internal resistance is in favor of increasing the working voltage. Thus, the nickel electrodes added with Co–Al–LDH have higher working voltage. Meanwhile, in Fig. 4b, the discharge platform voltage of the electrode B is 1.29 V. Compared with the other nickel electrodes added with Co–Al–LDH, the discharge platform voltage of the electrode B is highest. The reason is that Co/Al = 4:1 (molar ration) Co–Al–LDH possesses the appropriate Al(OH)$_3$ content. In general, the pure CoOOH is short of electrical conductivity because of the loose crystal. The appropriate content of Al(OH)$_3$ can take the place of a part of the CoOOH molecular, form the compact phase and improve the electrical conductivity. Thus, the discharge platform voltage for the nickel electrode added with Co/Al = 4:1 (molar ration) Co–Al–LDH is the highest among the nickel electrodes added with Co–Al–LDH.

In Fig. 4b, the discharge plateau voltage of the nickel electrode added with Co/Al = 4:1 (molar ration) Co–Al–LDH is a little higher than the nickel electrode added with CoO. The reason should be that Co–Al–LDH has a greater ability to improve conductivity. In the structure of Co–Al–LDH, Al^{3+} is embedded into the crystal lattice of Co(OH)$_2$ and the extra Al^{3+} is good to form CoOOH compact phase during the activity process. The compact phase is better than the flimsy layer composed of Co$_3$O$_4$ in improving the conductivity of the Ni(OH)$_2$ particles [1]. Thus, the nickel electrode added with Co/Al = 4:1 (molar ration) Co–Al–LDH has a higher discharge platform voltage.

Fig. 5 displays the charge–discharge cycle performance of the nickel electrodes added with different Co/Al molar ratios Co–Al–LDH, the pure nickel electrode and the nickel electrode added with CoO. As seen in Fig. 5, the stability of the nickel electrode added with Co–Al–LDH is better than the pure nickel electrode. The reason is that the additive of cobalt compound can inhibit the formation of γ-NiOOH [10]. In general, during the charge process, especially during overcharge, the product β-NiOOH can be easily transformed into γ-NiOOH. But γ-NiOOH can cause swelling and
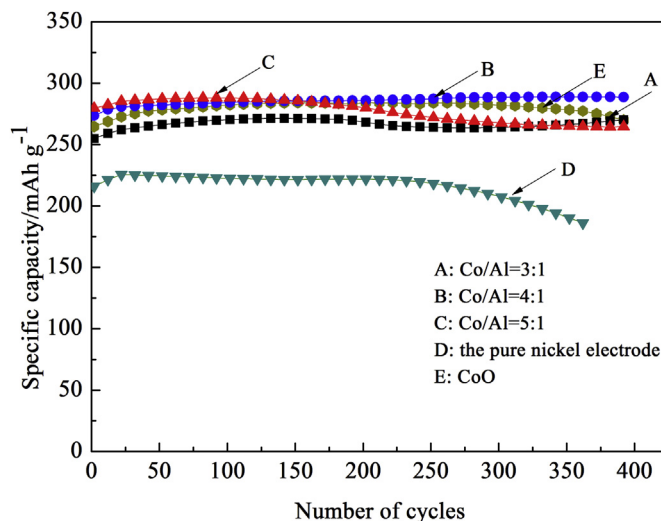

Fig. 5. The variation of the specific capacity with the number of cycles for the Ni–MH with (A) the nickel electrode added with Co/Al = 3:1 (molar ration) Co–Al–LDH; (B) the nickel electrode added with Co/Al = 4:1 (molar ration) Co–Al–LDH; (C) the nickel electrode added with Co/Al = 5:1 (molar ration) Co–Al–LDH; (D) the pure nickel electrode and (E) the nickel electrode added with CoO.

blistering of the electrode and result in the degradation of the electrode [26]. Thus, the additive Co–Al–LDH is in favor of keeping the stability of the nickel electrode., Fig. 5 also shows the specific capacity of the electrode A, B and C is 260, 283 and 275 mAh g⁻¹, respectively, after 200th cycles. It is higher than the specific capacity of the electrode D which is 250 mAh g⁻¹. The reason is that the conductivity of CoOOH is better than Ni(OH)$_2$ and NiOOH. It improves the electrical conductivity among Ni(OH)$_2$ particles, increases utilization of active materials and energy conversion efficiency. And, in Fig. 5, the specific capacity for the electrode B is always increasing along with the increasing cycle number and up to 287 mAh g⁻¹ at 400th cycle. It results from that Co–Al–LDH has a further activation. During the charge process, Co(OH)$_4^{2-}$ firstly is oxidized into CoOOH, the reaction equation is as follows:

$$Co(OH)_4^{2-} = CoOOH + H_2O + OH^- + e \qquad (8)$$
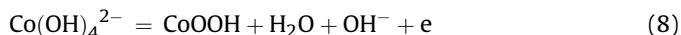
But the above reaction can't be sufficient. With the cycle number increasing, the content of CoOOH is more and more and the conductivity of the nickel electrode added with Co–Al–LDH is further improved. So the charge–discharge efficiency increases along with a further activation of Co–Al–LDH. Fig. 5 also shows the specific capacity of the nickel electrode added with CoO is 282 mAh g⁻¹ which is higher than the pure electrode. And, the stability of this electrode is also better than the pure nickel electrode. The reason is that the formed Co$_3$O$_4$ improves the conductivity [1] and inhibits the formation of γ-NiOOH. But the stability for the nickel electrode added with CoO is not as good as the nickel electrode added with Co/Al = 4:1 (molar ration) Co–Al–LDH. It results from the special layer structure of Co–Al–LDH is more stable in the electrolyte. The stable structure avoids the CoOOH transfer and is better able to inhibit the formation of γ-NiOOH. Thus, the stability of the nickel electrode added with Co/Al = 4:1 (molar ration) Co–Al–LDH is better.

3.5. The electrochemical impedance spectroscopes of the different nickel electrodes

In order to further study the influence of adding Co–Al–LDH, EIS measurements were performed and the impedance diagrams were
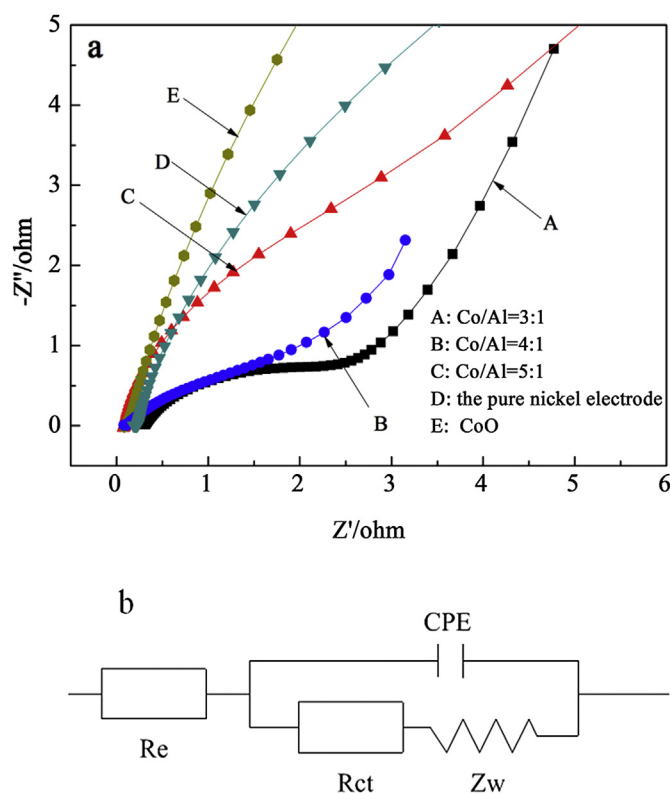
Fig. 6. Nyquist plots of the nickel electrodes (a): (A) the nickel electrode added with Co/Al = 3:1 (molar ration) Co—Al-LDH; (B) the nickel electrode added with Co/Al = 4:1 (molar ration) Co—Al-LDH; (C) the nickel electrode added with Co/Al = 5:1 (molar ration) Co—Al-LDH; (D) the pure nickel electrode; (E) the nickel electrode added with CoO and the equivalent circuit model for the EIS spectrum (b).

displayed in Fig. 6a, and the relevant fitting equivalent circuit was also shown in Fig. 6b. As seen in Fig. 6a.

Nyquist plots contain capacitive semicircular loop at high-frequency range and straight line in low-frequency part. The capacitive semicircular loop is attributed to the charge-transfer resistance in parallel with the double-layer capacitance and the straight line represents the diffusion process of OH^- in the nickel electrodes. As can be seen in Fig. 6b, CPE represents the constant phase element for a porous electrode, R_{ct} is the charge-transfer resistance, R_e is the ohmic resistance containing the resistance of the current collector, electrolyte, electrode materials, etc, and Z_W is the Warburg impedance. The R_e and R_{ct} for the different nickel electrodes are listed in Table 1. In Table 1, the corresponding R_{ct} is 0.3961, 0.2238, 0.5573 Ω and the R_e is 0.1976, 0.1768, 0.2397 Ω, respectively, for the electrode A, B and C. It is lower than the pure nickel electrode (0.8972, 0.2473 Ω). The lower R_{ct} indicates that the electrochemical reaction is easier, which is in accord with Fig. 3. The possible reason is that Co—Al-LDH has better ability to transfer proton, promote charge transfer between active material and

Table 1
The date of the EIS curves for the nickel electrode: (A) the nickel electrode added with Co/Al = 3:1 (molar ration) Co—Al-LDH; (B) the nickel electrode added with Co/Al = 4:1 (molar ration) Co—Al-LDH; (C) the nickel electrode added with Co/Al = 5:1 (molar ration) Co—Al-LDH; (D) the pure nickel electrode and (E) the nickel electrode added with CoO.

Sample	R_e (Ω)	R_{ct} (Ω)
A	0.1976	0.3961
B	0.1768	0.2238
C	0.2379	0.5573
D	0.2473	0.8972
E	0.1076	0.8865

electrolyte. And, the $Co(OH)_4^{2-}$ can be oxidized into CoOOH which has higher conductivity than $Ni(OH)_2$ and NiOOH, provide a good electrical path between the nickel hydroxide particles and the foamed-Ni substrate, thus the lower R_e for the electrode A, B and C is gained. Meanwhile, in Table 1, the R_e and R_{ct} for the nickel electrode added with CoO is also obtained. The R_e for the nickel electrode added with CoO is smaller than the nickel electrode added with Co—Al-LDH. It indicates Co—Al-LDH is not equal to CoO in terms of decreasing the ohmic resistance. But the R_{ct} for the nickel electrode added with Co—Al—LDH is smaller than the nickel electrode added with CoO. It shows the added Co—Al-LDH has a better effect in decreasing the charge-transfer resistance.

3.6. The rate capability of the Ni—MH cells with the different nickel electrodes

A high rate capability is more important in meeting the needs of high-storage applications [31]. So it is important for the Ni—MH cell to improve the rate capability. In order to measure the rate capability of Ni—MH cells with the nickel electrode added with Co/Al = 4:1 (molar ration) Co—Al-LDH and the pure nickel electrode, the cells were cycled at various rate of 0.5 C, 1 C, 2 C, and 5 C. Fig. 7
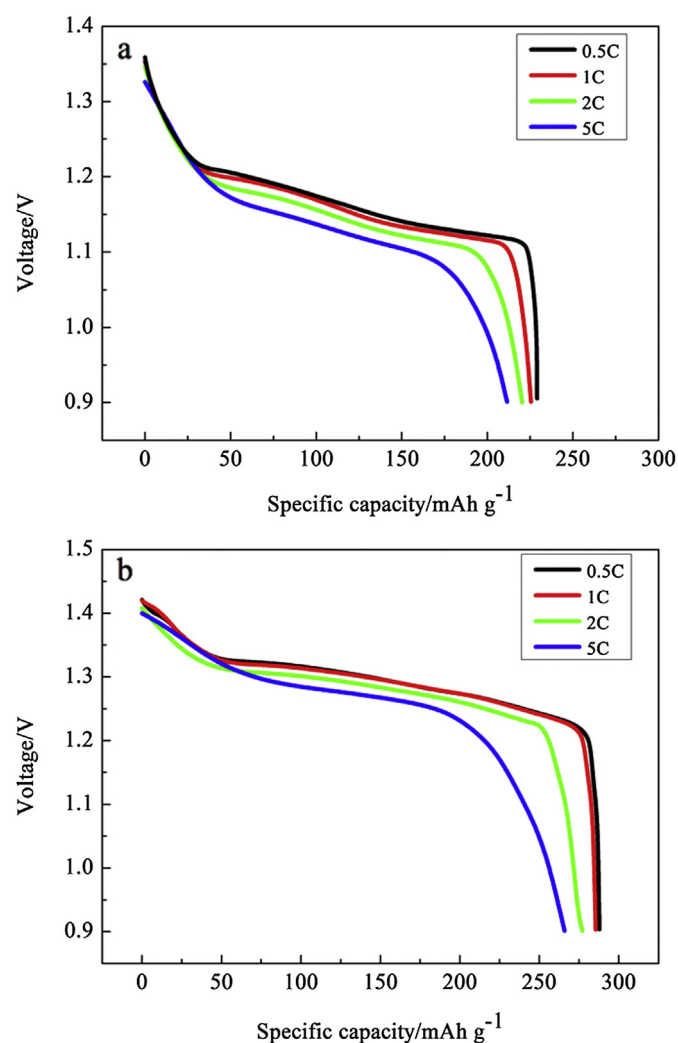

Fig. 7. The discharge curves for the MH—Ni cells at the different discharge currents: (a) the pure nickel electrode; (b) the nickel electrode added with Co/Al = 4:1 (molar ration) Co—Al-LDH.

shows the tenth discharge curves of the pure nickel electrode and the nickel electrode added with Co/Al = 4:1 (molar ration) Co–Al-LDH at the different discharge rate. From Fig. 7 can be seen, the discharge voltage platform of the nickel electrode is decreasing with increasing of the discharge rate. The reason is that the polarization of nickel electrode is increased with increasing of the current. Meanwhile, the discharge voltage platform and the specific capacity for the nickel electrode added with Co/Al = 4:1 (molar ration) Co–Al-LDH is higher than the pure nickel electrode at the same discharge rate. The excellent rate capability for the nickel electrode added with Co/Al = 4:1 (molar ration) Co–Al-LDH can result from CoOOH enhances the conductivity of the active material, decreases the resistance and the degree of polarization, improves the use ration of the active material. Thus, the added Co/Al = 4:1 (molar ration) Co–Al-LDH plays a good role in improving the rate capacity for the Ni–MH cell.

4. Conclusions

Co–Al–CO$_3$ layered double hydroxide (LDH) with the different Co/Al molar ration is synthesized by hydrothermal method and investigated as an additive for positive material of the Ni–MH cells. The structure of the Co–Al-LDH with different Co/Al molar ration is investigated. Meanwhile, the electrochemical performances of the nickel electrodes added with the different Co/Al molar ration Co–Al-LDH, the pure nickel electrode and the nickel electrode added with CoO are also studied. The Co/Al = 4:1 (molar ration) Co–Al-LDH possesses the best hexagonal crystal structure. Compared with the pure nickel electrode and the nickel electrode added with CoO, the nickel electrode added with Co/Al = 4:1 (molar ration) Co–Al-LDH has higher discharge capacity and more stable cycling performances. The cell can undergo at least 400 charge–discharge cycles at constant current of 1 C. The nickel electrode added with Co/Al = 4:1 (molar ration) Co–Al-LDH possesses a higher rate capability to meet the needs of high-storage applications. These results show Co–Al-LDH is a good additive for the nickel electrode.

Acknowledgments

References

[1] Y. Xia, Y. Yang, H. Shao, J. Power Sources 196 (2011) 495–503.
[2] C. Zhao, Y. Gu, H. Chen, Z. Jiang, Electrochim. Acta 47 (2002) 1801–1809.
[3] K. Provazi, M.J. Giz, L.H. Dall'Antonia, S.I. Córdoba de Torresi, J. Power Sources 102 (2001) 224–232.
[4] N. Furukawa, J. Power Sources 51 (1994) 45–59.
[5] W.H. Zhu, J.J. Ke, H.M. Yu, D.J. Zhang, J. Power Sources 56 (1995) 75–79.
[6] S.I.C. de Torresi, Electrochim. Acta 40 (1995) 1101–1107.
[7] A. Yuan, S. Cheng, J. Zhang, C. Cao, J. Power Sources 76 (1998) 36–40.
[8] S.N. Begum, V.S. Muralidharan, C. Ahmed Basha, Int. J. Hydrogen Energy 34 (2009) 1548–1555.
[9] F.Y. Cheng, J. Chen, P.W. Shen, J. Power Sources 150 (2005) 255–260.
[10] W. Li, S. Zhang, J. Chen, J. Phys. Chem. B 109 (2005) 14025–14032.
[11] A.H. Zimmerman, J. Power Sources 12 (1984) 233–245.
[12] R.D. Armstrong, E.A. Charles, J. Power Sources 27 (1989) 15–27.
[13] R.D. Armstrong, G.W.D. Briggs, E.A. Charles, J. Appl. Electrochem. 18 (1988) 215–219.
[14] J.B. Wu, J.P. Tu, X.L. Wang, W.K. Zhang, Int. J. Hydrogen Energy 32 (2007) 606–610.
[15] P. Elumalai, H.N. Vasan, N. Munichandraiah, J. Power Sources 93 (2001) 201–208.
[16] V. Pralong, A. Delahaye-Vidal, B. Beaudoin, B. Gerand, J.M. Tarascon, J. Mater. Chem. 9 (1999) 955–960.
[17] M. Ortiz, D. Becker, G. Garaventta, A. Visintin, E.B. Castro, S.G. Real, Electrochim. Acta 56 (2011) 7946–7954.
[18] Y. Xia, Y. Yang, H. Shao, Int. J. Hydrogen Energy 36 (2011) 8560–8569.
[19] F. Tronel, L. Guerlou-Demourgues, M. Ménétrier, L. Croguennec, L. Goubault, P. Bernard, C. Delmas, Chem. Mater. 18 (2006) 5840–5851.
[20] M. Douin, L. Guerlou-Demourgues, L. Goubault, P. Bernard, C. Delmas, J. Power Sources 193 (2009) 864–870.
[21] W. Chen, Y. Yang, H. Shao, J. Power Sources 196 (2011) 488–494.
[22] X. Fan, Z. Yang, R. Wen, B. Yang, W. Long, J. Power Sources 224 (2013) 80–85.
[23] X. Fan, Z. Yang, X. Xie, W. Long, R. Wang, Z. Hou, J. Power Sources 241 (2013) 404–409.
[24] R. Wang, Z. Yang, B. Yang, T. Wang, Z. Chu, J. Power Sources 251 (2014) 344–350.
[25] X. Fan, Z. Yang, W. Long, Z. Zhao, B. Yang, Electrochim. Acta 92 (2013) 365–370.
[26] A. Yuan, S. Cheng, J. Zhang, C. Cao, J. Power Sources 77 (1999) 178–182.
[27] C.C. Yang, Int. J. Hydrogen Energy 27 (2002) 1071–1081.
[28] F. Lichtenberg, K. Kleinsorgen, J. Power Sources 62 (1996) 207–211.
[29] W.K. Hu, X.P. Gao, M.M. Geng, Z.X. Gong, D. Noréus, J. Phys. Chem. B 109 (2005) 5392–5394.
[30] P. Benson, G.W.D. Briggs, W.F.K. Wynne-Jones, Electrochim. Acta 9 (1964) 275–280.
[31] T. Zhao, S. Chen, L. Li, X. Zhang, R. Chen, I. Belharouak, F. Wu, K. Amine, J. Power Sources 228 (2013) 206–213.